

Synthesis and Characterization of Diplatinum Complexes Containing Bridging $\mu\text{-}\eta^2\text{-H-SiHAr}$ Ligands. X-ray Crystal Structure Determination of $\{(\text{Ph}_3\text{P})\text{Pt}[\mu\text{-}\eta^2\text{-H-SiHAr}]\}_2$ (Ar = 2,4,6-(CF₃)₃C₆H₂, C₆Ph₅)

J. Braddock-Wilking,* Y. Levchinsky, and N. P. Rath

Department of Chemistry, University of Missouri–St. Louis, 8001 Natural Bridge Road, St. Louis, Missouri 63121

Received July 13, 2000

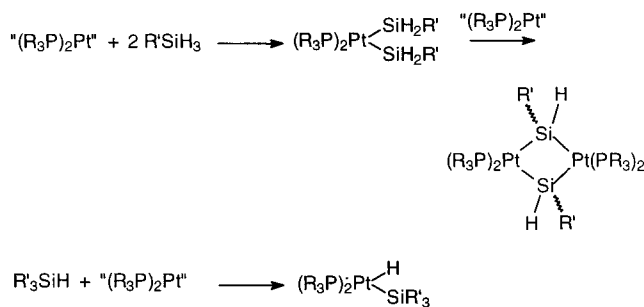
Dinuclear Pt–Si complexes, $[(\text{Ph}_3\text{P})\text{Pt}(\mu\text{-}\eta^2\text{-H-SiHAr})]_2$ (Ar = 2-isopropyl-6-methylphenyl (IMP), 2,4,6-trimethoxyphenyl (TMP), 2,4,6-trimethylphenyl (Mes), pentaphenylphenyl (PPP), 2,4,6-tris(trifluoromethyl)phenyl (R_F)) have been synthesized from the reaction of ArSiH_3 with $(\text{Ph}_3\text{P})_2\text{Pt}(\eta^2\text{-C}_2\text{H}_4)$. These complexes were characterized by multinuclear NMR and IR spectroscopy and X-ray crystallography (PPP and R_F systems). The dinuclear complexes contain a 3c–2e nonclassical interaction for $\text{Pt}\cdots\text{H}\cdots\text{Si}$, which is supported by spectroscopic and crystallographic data. Both cis and trans isomers are formed when Ar = IMP, TMP, Mes, and these complexes are fluxional on the NMR time scale. Only the trans isomer is generated with Ar = PPP, R_F. These complexes exhibit an unusual low-field ¹H NMR resonance for the terminal Si–H and an upfield shift for the bridging hydride. X-ray crystallographic analysis of the PPP and R_F systems (also previous results for IMP) reveal two different Si–Pt distances, with the longer distance corresponding to the $\text{Pt}\cdots\text{H}\cdots\text{Si}$ interaction.

Introduction

The study of complexes containing a transition-metal–silicon bond has grown significantly in the last two decades.¹ There are a variety of synthetic methods known for the formation of complexes containing a M–Si bond, but by far the most facile and versatile route involves addition of a Si–H bond in a hydrosilane to a transition-metal center. The reaction can proceed to the limit of full addition of the Si–H bond or may be “arrested” at an earlier stage to give a complex containing a “nonclassical” $\text{M}\cdots\text{H}\cdots\text{Si}$ interaction.^{1a,2} Silicon–hydrogen bond activation is implicated in a number of transition-metal-catalyzed reactions such as the interaction of hydrosilanes with transition metals in the formation of silicon oligomers and polymers (metal-catalyzed dehydrocoupling).³

The addition of a Si–H bond to a coordinatively unsaturated platinum(0) complex (i.e., $[\text{Pt}(\text{PR}_3)_2]$) can provide a variety of different products, depending upon

Scheme 1



the nature of the groups bound to silicon and to platinum. Primary silanes containing moderately bulky ligands generally afford bis(silyl)platinum species (Pt-Si_2) or dinuclear Pt_2Si_2 complexes that contain bridging silylene moieties ($\mu\text{-SiR}_2$).^{1,4,5} The bis(silyl)platinum complexes have been proposed as precursors to dinuclear Pt_2Si_2 complexes.⁴ However, tertiary silanes (and some secondary silanes) generally yield mononuclear complexes such as $\text{L}_2\text{Pt}(\text{H})\text{Si}$ (L = phosphine; Scheme 1).¹ Hydridoplatinum silyl complexes prepared from primary silanes are rare.

A number of complexes are known which contain bridging silylene units ($\mu\text{-SiR}_2$) between two metals (metals in groups 4 and 6–10).⁵ Several of these

* To whom correspondence should be addressed. Tel: (314) 516-6436. Fax: (314) 516-5342. E-mail: jwilking@umsl.edu.

(1) (a) Corey, J. Y.; Braddock-Wilking, J. *Chem. Rev.* **1999**, *99*, 175. (b) Eisen, M. S. In *The Chemistry of Organic Silicon Compounds*; Rappoport, Z., Apeloig, Y., Eds.; Wiley: New York, 1998; Vol. 2, p 2037. (c) Tilley, T. D. In *The Silicon Heteroatom Bond*; Patai, S., Rappoport, Z., Eds.; Wiley: New York, 1991; p 245. (d) Tilley, T. D. In *The Chemistry of Organic Silicon Compounds*; Patai, S., Rappoport, Z., Eds.; Wiley: New York, 1989; p 1416. (e) Aylett, B. J. *Adv. Inorg. Chem. Radiochem.* **1982**, *25*, 1.

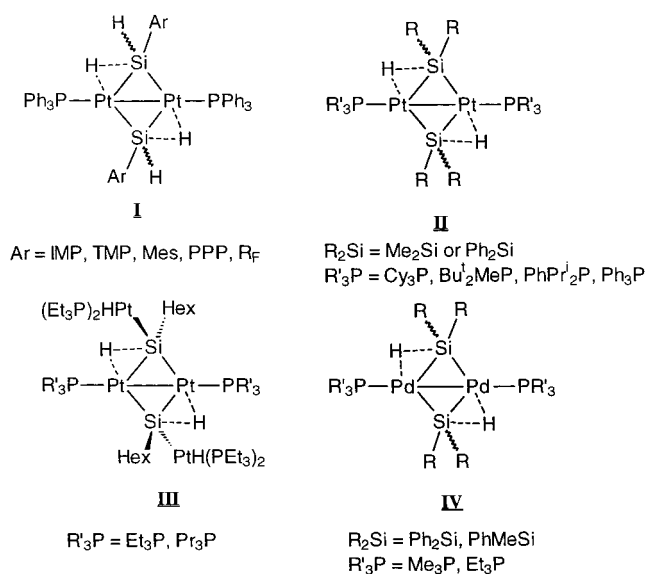
(2) Schubert, U. *Adv. Organomet. Chem.* **1990**, *30*, 151.

(3) (a) Gauvin, F.; Harrod, J. F.; Woo, H. G. *Adv. Organomet. Chem.* **1998**, *42*, 363. (b) Yamashita, H.; Tanaka, M. *Bull. Chem. Soc. Jpn.* **1995**, *68*, 403. (c) Tilley, T. D. *Acc. Chem. Res.* **1993**, *26*, 22. (d) Corey, J. Y. *Adv. Silicon Chem.* **1991**, *1*, 327. (e) Tilley, T. D. *Comments Inorg. Chem.* **1990**, *10*, 37. (f) Curtis, M. D.; Epstein, P. S. *Adv. Organomet. Chem.* **1981**, *19*, 213.

(4) (a) Shimada, S.; Tanaka, M.; Honda, K. *J. Am. Chem. Soc.* **1995**, *117*, 8289. (b) Heyn, R. H.; Tilley, T. D. *J. Am. Chem. Soc.* **1992**, *114*, 1917. (c) Michalczyk, M. J.; Recatto, C. A.; Calabrese, J. C.; Fink, M. *J. Am. Chem. Soc.* **1992**, *114*, 7955.

(5) (a) Ogino, H.; Tobita, H. *Adv. Organomet. Chem.* **1998**, *42*, 223. (b) Braddock-Wilking, J.; Levchinsky, Y.; Rath, N. P. Submitted for publication.

Chart 1



bridging silylene complexes also possess a hydrogen that bridges the metal and the silicon. The majority of the examples are from metals of the middle to late transition series (i.e., Ru, Rh, Pt).^{5a} Complexes containing platinum triad metals that possess a nonclassical $M\cdots H\cdots Si$ (3c–2e) interaction are rare. Stone and co-workers prepared a number of complexes with the general formula $[(R'_3P)Pt(\mu\text{-}\eta^2\text{-H-SiR}_2)]_2$ (**II** in Chart 1; $R'_3P = Cy_3P, Bu_2MeP, PhPr_2P, Ph_3P$; $SiR_2 = SiMe_2, SiPh_2$) from the reaction of $(R'_3P)Pt(\eta^2\text{-C}_2H_4)_2$ with $R_2\text{-SiH}_2$ at room temperature.⁶ Tessier et al. recently reported the formation of several diplatinum complexes, two of which contain $Pt\cdots H\cdots Si$ interactions as in $\{(R_3P)Pt[\mu\text{-}\eta^2\text{-H-Si(Hex)(Pt(PR}_3)_2H)]\}_2$ (**III** in Chart 1; $R = Et, Pr$).⁷ Kim and Osakada have prepared several dipalladium systems of the general formula $[(L)Pd(\mu\text{-}\eta^2\text{-H-SiR}_2)Pd(L)_n]$ (where $L = PMe_3, PET_3, PMePh_2$, $R = Ph$ ($n = 1$ (**IV** in Chart 1; and also $n = 2$ for PMe_3); $L = PMe_3$, or PET_3 , $SiR_2 = SiMePh$, $n = 1$; **IV** in Chart 1) that contain $Pd\cdots H\cdots Si$ interactions.⁸

Confirmation of a $M\cdots H\cdots Si$ interaction is customarily obtained by X-ray crystallography and/or 1H NMR spectroscopy. Elongated $M\cdots H$, $Si\cdots H$, and $M\cdots Si$ distances are expected in a nonclassical interaction. However, these key distances may not provide conclusive evidence for the presence of a $M\cdots H\cdots Si$ interaction, since hydrides are often difficult to locate by X-ray crystallography and their distances are sometimes approximate. The average Si–H distance in an organosilane is usually set at 1.5 Å.⁹ Schubert has suggested an upper limit of 2.0 Å for any interaction between Si and H.² In addition, M–Si distances can vary over a wide range and the 3c–2e distances overlap the range

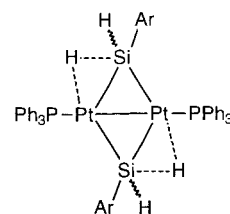
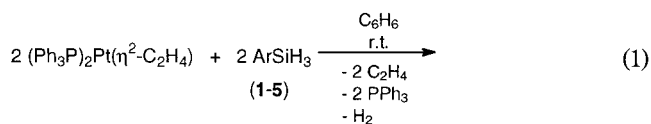
defined by 2c–2e M–Si bond distances.¹ A more reliable technique for establishing the presence of a $M\cdots H\cdots Si$ interaction is by 1H NMR spectroscopy. A substantial lowering of the $^1J_{SiH}$ coupling constant (20–100 Hz vs $\sim 150\text{--}200$ Hz for a normal Si–H bond) is observed for complexes containing a $M\cdots H\cdots Si$ interaction.^{1a,2}

Recently, we reported the preparation of the dinuclear platinum complex $[(Ph_3P)Pt(\mu\text{-}\eta^2\text{-H-SiH(IMP)})_2]$ (IMP = 2-isopropyl-6-methylphenyl), which contains a nonclassical $Pt\cdots H\cdots Si$ interaction.¹⁰ In our continued efforts to understand the steric and electronic factors that influence the Si–H addition to metals, we examined the reactivity of several bulky primary silanes with selected Pt(0) precursors. Herein, we report the stoichiometric reactions of the sterically hindered arylsilanes $ArSiH_3$ ($Ar = 2\text{-isopropyl-6-methylphenyl}$ (IMP, **1**),¹⁰ 2,4,6-trimethoxyphenyl (TMP, **2**),¹¹ 2,4,6-trimethylphenyl (Mes, **3**),¹² 2,3,4,5,6-pentaphenylphenyl (PPP, **4**),¹³ 2,4,6-tris(trifluoromethyl)phenyl (R_F , **5**)¹⁴) with $(Ph_3P)_2Pt(\eta^2\text{-C}_2H_4)$, which provided the dinuclear complexes $[(Ph_3P)Pt(\mu\text{-}\eta^2\text{-H-SiH(Ar)})_2]$ (**6–10**), respectively. All of these new derivatives contain a nonclassical 3c–2e interaction involving platinum, hydrogen, and silicon ($Pt\cdots H\cdots Si$).

Results

Synthesis and Spectroscopic Characterization.

Reaction of $(Ph_3P)_2Pt(\eta^2\text{-C}_2H_4)$ with 1 equiv of $ArSiH_3$ (**1–5**) in benzene (or toluene) solutions at room temperature afforded complexes of the general formula $\{(Ph_3P)Pt[\mu\text{-}\eta^2\text{-H-SiH(Ar)}]\}_2$ (**6–10**) in good yield (69–97% for **6–9**, 19% for **10**). Complexes **6–8** were isolated as a mixtures of trans (**6a–8a**) and cis (**6b–8b**) isomers (in a ratio of 3:1 for **6**; 3:2 for both **7** and **8**)¹⁵ (eq 1).



Ar = IMP (**6**), TMP (**7**), Mes (**8**)
 PPP(**9**), R_F (**10**)

Complexes **9** and **10** were isolated as the trans isomer only. The reaction occurred instantly for silanes **1–3** (but more slowly for **4** and **5**) with vigorous gas evolution followed by rapid precipitation of the microcrystalline

(6) Auburn, M.; Ciriano, M.; Howard, J. A. K.; Murray, M.; Pugh, N. J.; Spencer, J. L.; Stone, F. G. A.; Woodward, P. *J. Chem. Soc., Dalton Trans.* **1980**, 659.

(7) Sanow, L. M.; Chai, M.; McConville, D. B.; Galat, K. J.; Simons, R. S.; Rinaldi, P. L.; Youngs, W. J.; Tessier, C. A. *Organometallics* **2000**, *19*, 192.

(8) (a) Kim, Y.-J.; Lee, S.-C.; Park, J.-I.; Osakada, K.; Choi, J.-C.; Yamamoto, T. *Organometallics* **1998**, *17*, 4929. (b) Kim, Y.-J.; Lee, S.-C.; Park, J.-I.; Osakada, K.; Choi, J.-C.; Yamamoto, T. *J. Chem. Soc., Dalton Trans.* **2000**, 417.

(9) See footnote 8 in: Kawachi, A.; Tanaka, Y.; Tamao, K. *Organometallics* **1997**, *16*, 5102.

(10) Levchinsky, Y.; Rath, N. P.; Braddock-Wilking, J. *Organometallics* **1999**, *18*, 2583.

(11) Levchinsky, Y.; Rath, N. P.; Braddock-Wilking, J. *J. Organomet. Chem.* **1999**, *588*, 51.

(12) (a) Malisch, W.; Hindahl, K.; Käß, H.; Reising, J.; Adam, W.; Precht, F. *Chem. Ber.* **1995**, *128*, 963. (b) Söldner, M.; Sandor, M.; Schier, A.; Schmidbaur, H. *Chem. Ber./Recl.* **1977**, *130*, 1671.

(13) Generously provided by Professor Peter P. Gaspar and Mark Autry, Washington University, St. Louis, MO.

(14) Molander, G. A.; Corrette, C. P. *Organometallics* **1998**, *17*, 5504.

(15) The ratio of isomers was determined from the relative intensities of the Si–H resonances in the 1H NMR spectrum.

Table 1. Selected NMR Spectroscopic Data for 6–10

Ar	$^1\text{H}(\text{Pt}\cdots\text{H}\cdots\text{Si})^a$		$^1\text{H}(\text{Si}-\text{H})^a$		$^{31}\text{P}\{^1\text{H}\}^a$	
	cis	trans	cis	trans	cis	trans
IMP (6) ¹⁰	2.17 ^{b-d}	2.17 ^{b,d,e}	8.42 $J = 137, 78^f$	8.92 $J = 216^g$ $J = 137, 72^f$	37.7 $J = 4279^h$ $J = 244^i$ $J = 60^j$	38.1 $J = 4276^h$ $J = 261^i$ $J = 60^j$
TMP (7)	2.38 ^d	2.44 ^d	8.65 $J = 160, 79^f$	8.95 $J = 159, 74^f$	41.2 $J = 4389^h$ $J = 278^i$ $J = 64^j$	41.0 $J = 4388^h$ $J = 285^i$ $J = 65^j$
Mes (8)	<i>k</i>	2.28 ^d	8.52 $J = 135, 73^f$	8.95 $J = 136, 75^f$	38.2 $J = 4264^h$ $J = 252^i$ $J = 60^j$	38.9 $J = 4250^h$ $J = 282^i$ $J = 60^j$
PPP (9)		0.35		7.48 $J = 48^g$ $J = 650^l$ $J = 112^f$ $J = 25^m$ $J = 7^n$		38.7 $J = 4368^h$ $J = 305^i$ $J = 63^j$
R _F (10)		2.10 ^d		8.41 ^d		35.9 $J = 4337^h$ $J = 216^i$ $J = 63^j$

^a Chemical shifts are given in ppm, and coupling constants are given in Hz. Spectra were obtained in C₆D₆. ^b Located by EXSY experiment. ^c 1.45 ppm in CD₂Cl₂. ^d *J* values are not resolved. ^e 1.49 ppm in CD₂Cl₂. ^f ²*J*_{PtH}. ^g ¹*J*_{SiH}. ^h ¹*J*_{PtP}. ⁱ ²*J*_{PtP}. ^j ³*J*_{PP}. ^k Obscured by other peaks. ^l ¹*J*_{PtH}. ^m ²*J*_{SiH}. ⁿ ²*J*_{PH}.

off-white product. Complex **6** could also be prepared from Pt(PPh₃)₄ in 70% yield, but the reaction proceeded at a slower rate (ca. 2 h).¹⁰ These solids are relatively air stable, as are solutions in either aromatic solvents or CD₂Cl₂ for several days or for months at -35 °C. However, fairly rapid decomposition in CDCl₃ and THF was observed. Complexes **6**¹⁰ and **7–10** were characterized by ¹H, ³¹P{¹H}, and ²⁹Si{¹H} NMR (¹H–²⁹Si HMQC), IR, and elemental analyses and, in some cases, 2D experiments (e.g., ¹H–¹H EXSY and ¹H–³¹P COSY), as well as X-ray crystallography (**6a**,¹⁰ **9**, and **10** only). Some of the most significant properties of **6–10** are found in the NMR and X-ray crystallographic data. These complexes showed several similar spectroscopic features; one complex will be described in detail, and the remaining NMR data are summarized in Table 1.

The ¹H NMR spectrum for **6–10** (C₆D₆) revealed terminal Si–H resonances at quite low field between ~8 and 9 ppm. The chemical shift for the terminal Si–H in **9** was obscured by aromatic resonances but was determined by a 2D ¹H–²⁹Si HMQC experiment (δ 7.48). For complexes **6–8** these resonances were flanked by two sets of Pt satellites, which confirmed inequivalent coupling of the terminal Si–H to each Pt center. Figure 1 shows the terminal (**7a,b** only) and bridging hydrides in the ¹H NMR spectrum (**7a,b** and **9**). Complex **10** showed a broad resonance for the terminal Si–H moiety, and coupling to Pt was not resolved. No coupling was observed between the terminal Si–H and the phosphorus atoms for **6–10**.

To the best of our knowledge, the chemical shifts for the terminal Si–H unit in **6–10** represent the most remote downfield resonances reported for a terminal Si–H group. In general, Si–H resonances appear between 3 and 5.5 ppm in the ¹H NMR spectrum for free hydrosilanes or M–Si–H species.^{1a,16} The bridging Pt···H···Si resonances of **6** and **8** were not resolved in benzene due to overlap with the Ar–Me resonances.

However, the chemical shift could be determined from the ¹H–¹H EXSY experiment. The ¹*J*_{SiH} coupling for the Pt···H···Si moiety for **6–8** and **10** could not be resolved due to overlapping resonances or extensive coupling to other nuclei. However, the bridging hydride in **9** was found at 0.35 ppm in the ¹H NMR spectrum as a doublet (coupling to ³¹P) with two sets of Pt and Si satellites with ¹*J*_{SiH} = 48 Hz (Table 1; Figure 1b).

The chemical shift assignment for the terminal and bridging hydrides was supported by deuterium labeling in **8-d₄**. For example, the terminal Si–H resonances for {(Ph₃P)Pt[μ-η²-H–SiH(Mes)]}₂ (**8**) were observed at 8.52 ppm (cis) and 8.95 ppm (trans) in the ¹H NMR spectrum. The bridging Pt···H···Si resonance of **8a** appeared at 2.27 ppm as a broad doublet between two Ar–Me peaks. The ¹H NMR spectrum of **8-d₄** was identical with the ¹H spectrum of **8**, except that the terminal and bridging hydride resonances were missing. On the other hand, the ²H NMR spectrum of **8-d₄** exhibited terminal and bridging deuterium resonances for both isomers of {(Ph₃P)Pt[μ-η²-D–SiD(Mes)]}₂ as broad peaks (2.28 and 8.93 ppm for **8a-d₄**; 1.49 and 8.51 ppm for **8b-d₄**). The one-bond platinum coupling, ¹*J*_{PtD}, was found to be 102 Hz, which corresponds to a ¹*J*_{PtH} value of 662 Hz.¹⁷ The value of the coupling constant supports the presence of a nonclassical 3c–2e interaction, since typical values for ¹*J*_{PtH} (where H is terminal) are typically greater than 800 Hz.¹⁸

A ¹H–¹H EXSY experiment revealed that **6–8** were fluxional on the NMR time scale at room temperature.

(16) Williams, E. A. In *The Chemistry of Organic Silicon Compounds*; Patai, S., Rappaport, Z., Eds.; Wiley: New York, 1989; Part 1, Chapter 8.

(17) The following equation was used to transform ¹*J*_{PtD} into ¹*J*_{PtH}: *J*_{HX}/*J*_{DX} = γ_{HX}/γ_{DX} (γ_{HX} = 26.7519; γ_{DX} = 4.1066): Silverstein, R. M.; Bassler, G. C.; Morrill, T. C. In *Spectroscopic Identification of Organic Compounds*, 5th ed.; Wiley: Toronto, Canada, 1991; p 187.

(18) Appleton, T. G.; Clark, H. C.; Manzer, L. E. *Coord. Chem. Rev.* **1973**, *10*, 335.

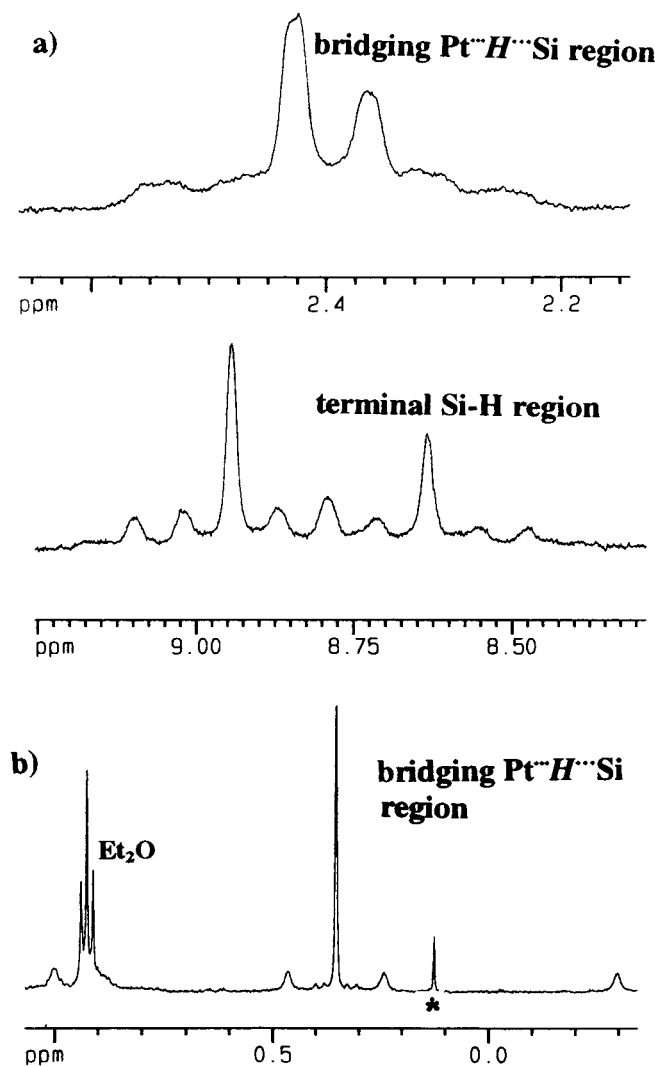


Figure 1. Selected 500 MHz (C_6D_6) ^1H NMR data for (a) compounds **7a,b** and (b) compound **9** ($\{^{31}\text{P}\}$ decoupled). The asterisk denotes an impurity.

Both terminal and bridging hydrides for each complex were found to undergo an exchange process with $\Delta G^\ddagger \approx 15\text{--}17$ kcal/mol,¹⁹ with coalescence temperatures of 342–356 K. These complexes are stable to brief heating to $\sim 80^\circ\text{C}$ and exhibit no change in the cis/trans ratio upon cooling to room temperature. The proposed mechanism for the fluxional process involves a simultaneous exchange of the terminal and bridging hydrides (Scheme 2) with concomitant cis–trans isomerization.

The ^{31}P NMR spectra of **6–10** exhibit part of an $\text{AA}'\text{XX}'$ spin system pattern for a dinuclear platinum complex containing one phosphine ligand at each metal center. Figure 2 shows the $^{31}\text{P}\{^1\text{H}\}$ NMR spectrum for **7a,b**. An intense central singlet (for each isomer) is observed near 40 ppm for those molecules containing no NMR-active ^{195}Pt nuclei. Each central line is flanked by two sets of Pt satellites that appear as doublets when

(19) The coalescence temperature was determined by studying the terminal Si–H region. It is assumed that **8-d₄** also undergoes the same isomerization process. The $^{31}\text{P}\text{--}^{31}\text{P}$ EXSY experiment for **7** showed a correlation between the cis and trans phosphorus resonances (see the Supporting Information). In addition, ^{31}P VT experiments revealed the same coalescence temperature and activation parameters within experimental error as observed in the ^1H VT NMR study. These data support the mechanism shown in Scheme 2.

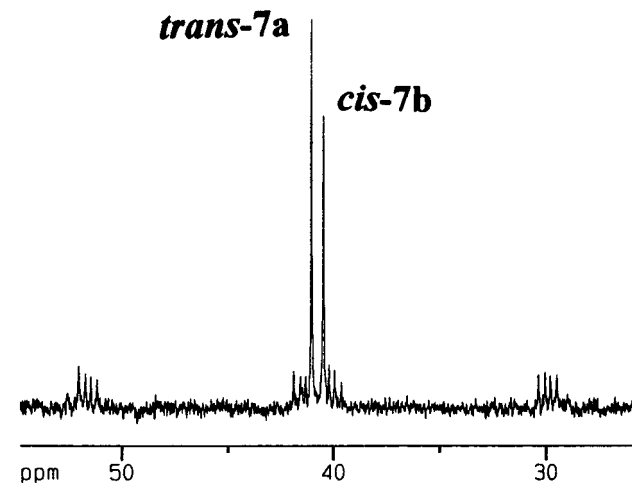
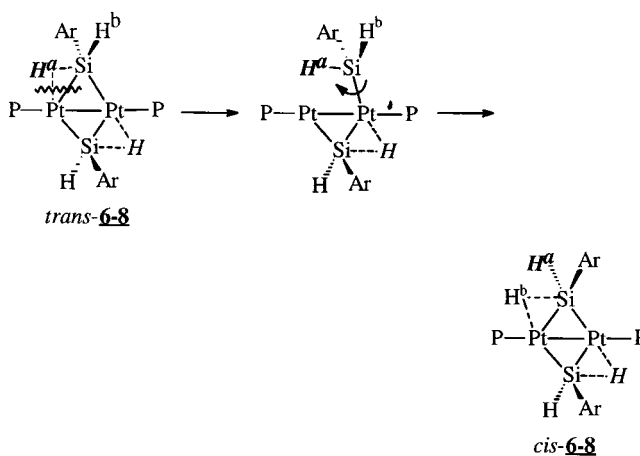


Figure 2. $^{31}\text{P}\{^1\text{H}\}$ NMR spectrum of **7** (202 MHz, C_6D_6).

Scheme 2



the molecule contains one ^{195}Pt nucleus. The multiplicity of the satellites is due to coupling between inequivalent phosphorus nuclei when one of the Pt nuclei is NMR active. Additionally, 10 more lines are expected for an $\text{AA}'\text{XX}'$ spin system when two ^{195}Pt nuclei are present; however, all 10 lines were not observed and thus the $^1J_{\text{PtPt}}$ value could not be measured.²⁰

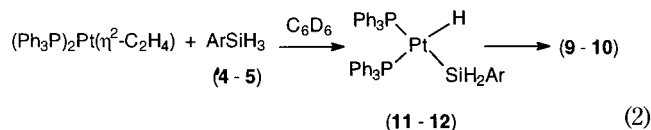
The ^{29}Si chemical shifts for **6–10** were measured from a $^1\text{H}\text{--}^{29}\text{Si}$ HMQC experiment and were found to be in the range of 125–175 ppm with the most downfield shift found for **9**. The ^{29}Si chemical shift values for **6–10** differ by ≥ 200 ppm relative to the corresponding free ArSiH_3 .²¹

The Si–H stretching frequency for **6–10** appeared in the infrared region as a strong band at $\sim 2100\text{ cm}^{-1}$, whereas the bridging hydride appeared as a broad band at $1620\text{--}1650\text{ cm}^{-1}$. **8-d₄** exhibited Si–D and $\text{Pt}\cdots\text{D}\cdots\text{Si}$ stretching frequencies at lower energies due to deuterium labeling. For example, the Si–H stretching vibration in **8** appeared as a strong band at 2122 cm^{-1} , whereas the corresponding Si–D band in **8-d₄** was observed at 1542 cm^{-1} .²² Similarly, the $\text{Pt}\cdots\text{H(D)}\cdots\text{Si}$ stretching bands were 1618 cm^{-1} for **8** and 1157 cm^{-1} for **8-d₄**.

(20) Kiffen, A. A.; Masters, C.; Visser, J. P. *J. Chem. Soc., Dalton Trans.* **1975**, 1311.

(21) For example, the ^{29}Si resonance for **4** appeared at -69.8 ppm (C_6D_6) (Braddock-Wilking, J.; Levchinsky, Y. Unpublished results) and -78.5 ppm for **1**.¹⁰

Initially, the reaction of $(\text{Ph}_3\text{P})_2\text{Pt}(\eta^2\text{-C}_2\text{H}_4)$ with 1 equiv of ArSiH_3 (**4** or **5**) at room temperature afforded the mononuclear species *cis*-(Ph_3P)₂Pt(H)[SiH₂Ar] (**11** and **12**, respectively) in quantitative yield by NMR spectroscopy (eq 2). The room-temperature conversions



of **11** to **9** and of **12** to **10** occurred with vastly different rates. For example, the conversion of **11** to **9** took place over approximately 3–4 h at room temperature (low yield) but was rapid at +78 °C in part due to the increased solubility of **11**. No Pt–Si-containing species other than **11** and **9** were observed in the reaction mixture. However, the formation of **10** took several months at room temperature (see below). No other intermediates, apart from complex **12**, were observed in the formation of **10**. Attempts to react $(\text{Ph}_3\text{P})_2\text{Pt}(\eta^2\text{-C}_2\text{H}_4)$ with excess $\text{R}_\text{F}\text{SiH}_3$ (**5**) in order to produce the bis(silyl) complex $(\text{Ph}_3\text{P})_2\text{Pt}[\text{SiH}_2(\text{R}_\text{F})]_2$ resulted in exclusive formation of **12**.

The formation of **11** and **12** was unexpected, due to the fact that complexes of the type $\text{L}_2\text{Pt}(\text{H})(\text{SiH}_2\text{R})$ are quite rare, and in general primary silanes react with phosphine–platinum precursors to give either bis(silyl) or dimeric species of the type $[(\text{R}_3\text{P})_2\text{Pt}(\mu\text{-SiHR})]_2$.¹ Surprisingly, there are no reports in the literature that describe the reactivity of $(\text{Ph}_3\text{P})_2\text{Pt}(\eta^2\text{-C}_2\text{H}_4)$ with primary silanes.¹ Complexes of this structural type are rare, and only a few examples are known, such as *trans*-(Cy_3P)₂Pt(H)(SiH₂Cl) and *trans*-(Cy_3P)₂Pt(H)(SiH₃).²³

Complexes **11** and **12** were characterized by ¹H, ²⁹Si{¹H}, and ³¹P{¹H} NMR and IR spectroscopy. In addition, solutions of **12** were analyzed by ¹⁹F NMR, several 2D COSY and EXSY experiments, and elemental analyses. Complexes **11** and **12** exhibited similar spectroscopic features, as discussed below.

The upfield region of the ¹H NMR spectrum (Figure 3) for **11** and **12** exhibited a doublet of doublets near –2 ppm flanked by ¹⁹⁵Pt satellites which arises from coupling to phosphorus nuclei *cis* and *trans* to the hydride (part of an AXX' system). Upon decoupling of the ³¹P nuclei, the doublet of doublets collapsed to a singlet with Pt–H coupling in the typical range for complexes of the type²⁴ $(\text{R}_3\text{P})_2\text{Pt}(\text{H})\text{PtSiR}_3$ ($^1J_{\text{PtH}} \approx 950$ Hz). The multiplicity pattern of the hydride, as well as the inequivalent coupling to the two phosphorus nuclei, indicated that the phosphines occupy mutually *cis* positions on the Pt center.

(22) These bands are related by a factor of 1.38, which is in good agreement with the theoretical value of 1.39: (a) Shoemaker, D. P.; Garland, C. W.; Nibler, J. W. In *Experiments in Physical Chemistry*, 6th ed.; McGraw-Hill: New York, 1996; p 400. (b) Ebsworth, E. A. V.; Rankin, D. W. H.; Craddock, S. In *Structural Methods in Inorganic Chemistry*, 2nd ed.; CRC Press: Boca Raton, FL, 1991; p 228.

(23) Ebsworth, E. A. V.; Marganian, V. M.; Reed, F. J. S.; Gould, R. O. *J. Chem. Soc., Dalton Trans.* **1978**, 1167.

(24) (a) Koizumi, T.; Osakada, K.; Yamamoto, T. *Organometallics* **1997**, *16*, 6014. (b) Latif, L. A.; Eaborn, C.; Pidcock, A.; Weng, N. S. *J. Organomet. Chem.* **1994**, *474*, 217. (c) Packett, D. L.; Syed, A.; Trogler, W. C. *Organometallics* **1988**, *7*, 159. (d) Paonessa, R. S.; Prigano, A. L.; Trogler, W. C. *Organometallics* **1985**, *4*, 647. (e) Ciriano, M.; Green, M.; Howard, J. A. K.; Proud, J.; Spencer, J. L.; Stone, F. G. A.; Tsipis, C. *J. Chem. Soc., Dalton Trans.* **1978**, 801.

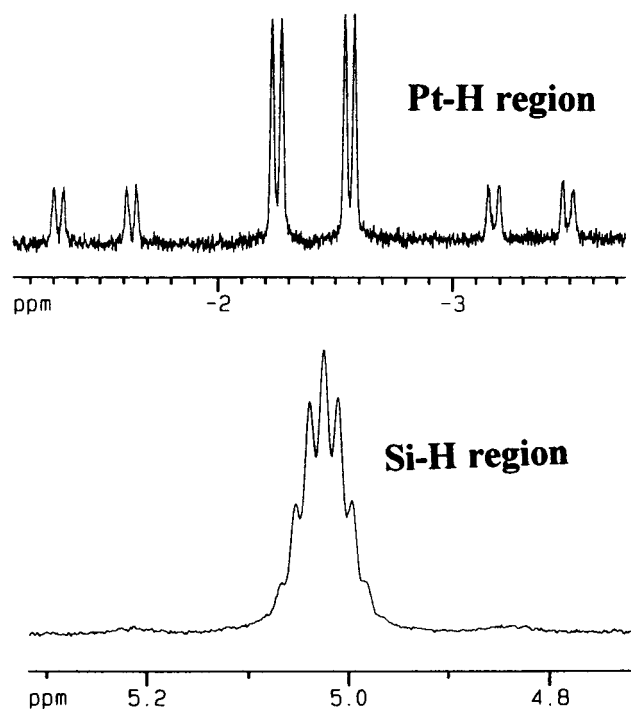


Figure 3. Selected ¹H NMR data (500 MHz, C₆D₆) for $(\text{Ph}_3\text{P})_2\text{Pt}(\text{H})[\text{SiH}_2(\text{R}_\text{F})]$ (**12**).

In contrast to **12**, which exhibited a Si–H resonance in the ¹H NMR spectrum (Figure 3) as a complex multiplet (δ 5.03) due to long-range fluorine coupling, the Si–H resonance of **11** appeared as a pseudo triplet centered at 4.26 ppm. The ¹H{³¹P} NMR spectrum for **11** showed the Si–H resonance as a sharp singlet without any observed coupling to platinum. This was unusual, because the Si–H resonance of **12** did couple to the Pt center ($^2J_{\text{PtH}} = 20$ Hz) but did not exhibit any coupling to phosphorus (confirmed by a ¹H–³¹P COSY experiment). These observations could be due to the difference in the electronic and steric effects between the R_F and PPP systems.

The ³¹P{¹H} NMR spectrum of **11** and **12** exhibited two doublets with Pt satellites near 30 ppm with similar Pt–P coupling ($^1J_{\text{PtP}} = 1713$ Hz for **11** and 1896 Hz for **12** (*P* *trans* to Si); $^1J_{\text{PtP}} = 2422$ Hz for **11** and 2282 Hz for **12** (*P* *trans* to H)). The ²⁹Si NMR spectrum of **11** and **12** showed a doublet of doublets upfield of TMS at –45 ppm flanked by platinum satellites. The resonance for **12** was broadened due to coupling to both ³¹P and ¹⁹F nuclei, and the coupling was not resolved, due to overlapping peaks. The magnitude of the downfield ²⁹Si shift for **11** and **12** is substantially smaller than the range seen for complexes **6–10** relative to the free silane.

The presence of both terminal Si–H (2089 cm^{–1} for **11**; 2126 cm^{–1} for **12**) and Pt–H groups (2068 cm^{–1} for **11**; 2072 cm^{–1} for **12**) was observed in the infrared spectrum. The higher energy Si–H stretching vibration for **12** can be explained on the basis of a higher concentration of “s” character in the Si–H bond.²⁵

In an effort to probe the mechanism of formation of **6–10**, we investigated the reactivity of a less hindered arylsilane, (*p*-Tol)SiH₃. Reaction of 2 equiv of (*p*-Tol)SiH₃ with 1 equiv of $(\text{Ph}_3\text{P})_2\text{Pt}(\eta^2\text{-C}_2\text{H}_4)$ proceeded

(25) Bent, H. A. *Chem. Rev.* **1961**, *61*, 275.

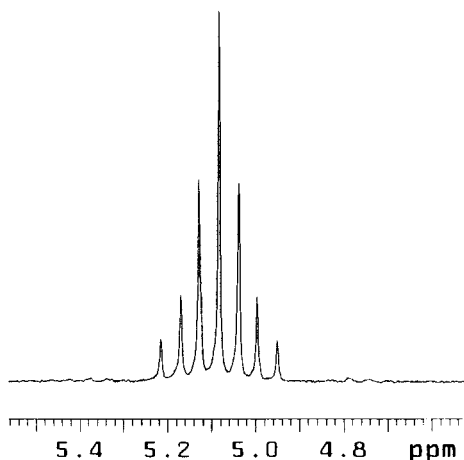
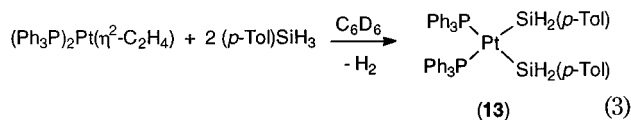


Figure 4. ^1H NMR spectrum (300 MHz, C_6D_6) showing the Si-H region of **13**.

rapidly with vigorous gas evolution to give *cis*-(Ph_3P) $_2$ -Pt[SiH $_2$ (*p*-Tol)] $_2$ (**13**) (quantitative yield by NMR) as a yellow solid (eq 3). Changing the ratio of starting



materials to 1:1 afforded **13** in 50% yield (based on the platinum precursor; all silane was consumed). The monosubstituted platinum complex (Ph_3P) $_2$ Pt(H)[SiH $_2$ (*p*-Tol)] was not observed by NMR spectroscopy. Interestingly, reaction of PhSiH_3 with (Ph_3P) $_2$ Pt(η^2 -C $_2$ H $_4$) gave several products.²⁶ Just after mixing, a short-lived species was observed by ^1H and $^{31}\text{P}\{^1\text{H}\}$ NMR that was assigned to (Ph_3P) $_2$ Pt(SiH $_2$ Ph) $_2$. In addition, a minor resonance was observed that was assigned to a dinuclear species analogous to **6–10**, [(Ph_3P)Pt(μ - η^2 -H-SiPh $_2$)] $_2$. No other Pt-Si-containing species were identified in the reaction mixture.

Complex **13** was characterized by ^1H and $^{31}\text{P}\{^1\text{H}\}$ NMR spectroscopy. The $^{31}\text{P}\{^1\text{H}\}$ spectrum exhibited a singlet centered at 35.5 ppm ($^1J_{\text{PtP}} = 1887$ Hz) flanked by platinum satellites. The value of the platinum-phosphorus coupling constant is consistent with a *cis* configuration for **13**.

The ^1H NMR spectrum of **13** exhibited a triplet Si-H resonance (with ^{195}Pt satellites) centered at 5.08 ppm with $^1J_{\text{SiH}} = 177$ Hz (Figure 4), a downfield shift of 0.8 ppm and a decrease by 22 Hz in $^1J_{\text{SiH}}$ for the free silane. The triplet arises from coupling to phosphorus, and platinum satellites overlap with the outer component of this triplet to give an overall appearance of a septet. The multiplet collapsed to a singlet flanked by Pt satellites upon decoupling of the ^{31}P nuclei. The upfield region of the ^1H spectrum of **13** did not exhibit any platinum-hydride resonances, thus confirming the bis(silyl) structure.

Complex **13** was found to be exceptionally light sensitive and underwent decomposition in toluene, hexane, and ether solutions. Bis(silyl)platinum complexes have been reported to decompose in benzene solutions.²⁷ It should be noted that complex **13** did not

Table 2. Crystal Data and Structure Refinement Details for **9 and **10****

	9	10
formula	$\text{C}_{72}\text{H}_{62}\text{P}_2\text{PtSi}$	$\text{C}_{36}\text{H}_{28}\text{F}_9\text{P}_2\text{PtSi}$
fw	1181.37	885.73
temp (K)	223(2)	223(2)
cryst dimens (mm)	$0.40 \times 0.18 \times 0.04$	$0.08 \times 0.14 \times 0.3$
cryst syst	triclinic	triclinic
space group	$P\bar{1}$	$P\bar{1}$
<i>a</i> (Å)	12.3883(2)	8.3309(1)
<i>b</i> (Å)	14.9728(2)	13.9395(2)
<i>c</i> (Å)	17.0647(2)	15.5969(2)
α (deg)	82.05(1)	74.832(1)
β (deg)	74.747(1)	82.811(1)
γ (deg)	67.47(1)	82.184(1)
<i>V</i> (Å 3)	2818.15(7)	1724.29(4)
<i>Z</i>	2	2
d_{calcd} (Mg/m 3)	1.392	1.706
μ (mm $^{-1}$)	2.582	4.224
GOF	1.008	1.029
R1 (obsd data)	0.0561	0.0356
wR2 (all data)	0.1407	0.0674
largest diff peak (e Å $^{-3}$)	2.423	1.261

Table 3. Selected Bond Lengths (Å) and Angles (deg) for **6a, **9**, and **10****

	6a ¹⁰	9	10
Bond Distances			
Pt-P	2.2485(8)	2.258(2)	2.2635(10)
Pt-Si	2.3248(9)	2.321(2)	2.2998(11)
	2.4280(9)	2.428(2)	2.4051(11)
Pt-Pt#1	2.7021(2)	2.7144(6)	2.7181(3)
Si-H (terminal)	1.593		1.445
Si...H (bridging)	1.669	1.647	
Pt...H	1.799	1.738	
Bond Angles			
Si-Pt-Si	110.74(3)	110.32(6)	109.46(3)
Pt-Si-Pt	69.26(3)	69.68(6)	70.54(3)
P-Pt-Si	105.08(3)	105.10(8)	106.63(4)
	143.89(3)	144.58(7)	143.47(4)
P-Pt-Pt	161.78(2)	162.10(5)	162.39(3)
Si-Pt-Pt	53.57(2)	53.32(5)	52.92(3)
	57.17(2)	57.00(6)	56.54(3)

seem to convert to the dimeric μ -silylene complex {(Ph_3P) $_2$ Pt[μ -HSi(*p*-Tol)]} $_2$, in contrast to {(Et $_3$ P) $_2$ Pt[SiH $_2$ (*p*-Tol)]} $_2$.²⁸ Complex **13** appears to be fairly stable in the solid state when stored in the dark.

X-ray Crystallography. The molecular structures of **6a**,¹⁰ **9**, and **10** were determined by X-ray crystallography. Crystal data and structure refinement for **9** and **10** are given in Table 2. For comparison, selected bond distances and angles for **6a**¹⁰ and **9** and **10** are given in Table 3. The molecular structures of **9** and **10** are shown in Figures 5 and 6, respectively. The central core structure of **6a** is shown in Figure 7. Both the terminal and bridging hydrides on silicon and platinum were located and refined for **6a**, but only the bridging hydrides for **9** and terminal hydrides for **10** were found. All three complexes exhibited a planar Pt $_2$ Si $_2$ core with the substituents at silicon lying directly above and below the plane of the ring. The phenyl groups on the pentaphenylphenyl moiety in complex **9** are oriented in a propeller type arrangement. Several similarities in the structures are observed between **6a** and complexes **9** and **10** and are summarized below.

A notable feature in the X-ray structures of **6a** and complexes **9** and **10** are two different Pt-Si distances

(27) Eaborn, C.; Ratcliff, B.; Pidcock, A. *J. Organomet. Chem.* **1974**, *65*, 181.

(28) Heyn, R. H.; Tilley, T. D. *J. Am. Chem. Soc.* **1992**, *114*, 1917.

(26) Braddock-Wilking, J.; Levchinsky, Y. Unpublished results.

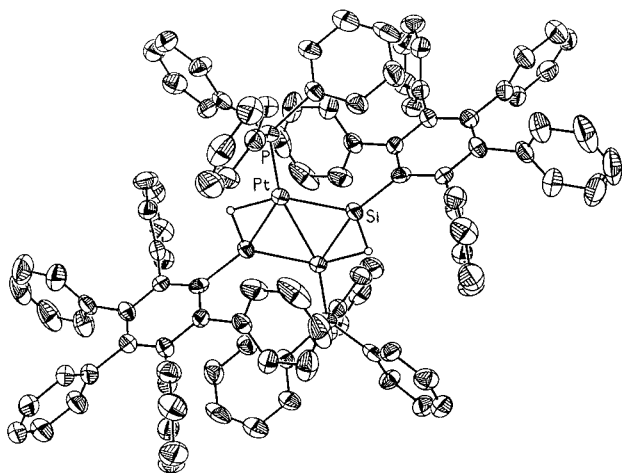


Figure 5. Molecular structure of $\{(\text{Ph}_3\text{P})\text{Pt}[\mu\text{-}\eta^2\text{-H-SiH(PPP)}]\}_2$ (**9**) with thermal ellipsoids drawn at 50% probability. Phenyl hydrogen atoms have been omitted for clarity.

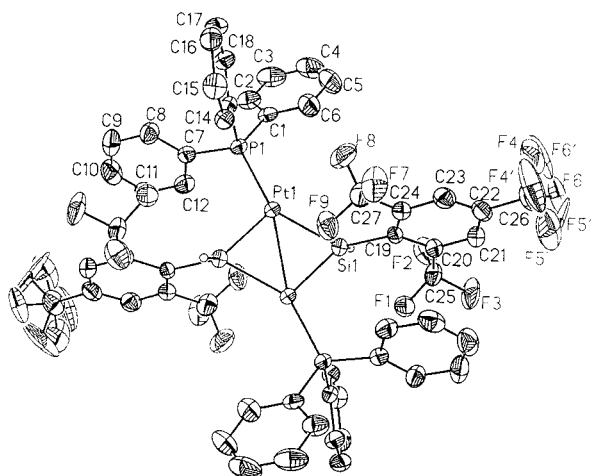


Figure 6. Molecular structure of $\{(\text{Ph}_3\text{P})\text{Pt}[\mu\text{-}\eta^2\text{-H-SiH(RF)}]\}_2$ (**10**) with thermal ellipsoids drawn at 50% probability. Phenyl hydrogen atoms have been omitted for clarity. The *p*-CF₃ groups are disordered.

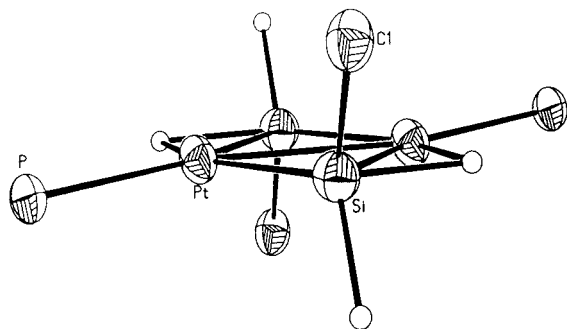


Figure 7. Partial molecular structure of **6a** showing the central core (thermal ellipsoids drawn at 50% probability).

(Table 3) with the shorter Pt–Si distance corresponding to the unbridged Pt–Si bond (~ 2.3 vs 2.4 Å). This is consistent with what is observed for complexes containing nonclassical interactions for $\text{M}\cdots\text{H}\cdots\text{Si}$, where elongated $\text{M}\cdots\text{H}$, $\text{Si}\cdots\text{H}$, and $\text{M}\cdots\text{Si}$ distances are expected, compared to normal $2c\text{-}2e$ bonds between these elements.^{1a,2} In addition, two different Pt–Si distances are consistent with the two distinct values of $^2J_{\text{PtSiH}}$ that were observed in the ^1H NMR spectrum. The Pt–Si

distances in **6a** and complexes **9** and **10** fall in the range of known Pt–Si bonds (mean value 2.368 Å).^{1a} Slightly shorter Pt–Si distances in **10** relative to **6a** and **9** are probably due to the stronger Pt–Si bonds found in complexes where a Si center contains electronegative substituents, such as the R_F ligand.¹

The Pt–Pt distances in **9** and **10** were found to be slightly longer than in **6a** ($2.7144(6)$, $2.7181(3)$, and $2.7021(2)$ Å, respectively). Despite the fact that the Pt–Pt distances are longer than the sum of the covalent radii (2.62 Å), they fall within the range of known values for two Pt(I) atoms bound to each other.²⁹ Each platinum atom in **6a** and in **9** and **10** has a distorted (due to the bridging hydride) square planar environment and a nonlinear P–Pt–Pt#1 angle of $\sim 162^\circ$. The obtuse Si–Pt–Si angles in **6a** and in **9** and **10** (ca. 110°) are consistent with a Pt–Pt bond. Consequently, the Pt–Si–Pt angles are acute ($\sim 70^\circ$).

Direct comparison of the terminal Si–H and bridging Si \cdots H distances was only possible for compound **6a** (1.593 vs 1.669 Å, respectively), where both types of hydrides were located. The elongated Si–H bridging vs terminal distance supports the presence of a nonclassical $3c\text{-}2e$ interaction. The bridging Si \cdots H distance in **9** and terminal Si–H distance in **10** are in good agreement with the values found for **6a** (Table 3). In addition, the Pt \cdots H distances in **6a** and **9** are slightly longer than normal.³⁰

Discussion

The present work has shown that bulky primary arylsilanes containing ortho substituents on the aromatic ring react with $(\text{Ph}_3\text{P})_2\text{Pt}(\eta^2\text{-C}_2\text{H}_4)$ to provide dinuclear complexes **6–10**. Spectroscopic and crystallographic data indicate that the same structure is present both in solution and in the solid state. Several notable features are found in solution and are discussed below. Many of these features are also found with the related derivatives prepared by Stone,⁶ Tessier,⁷ and Osakada.⁸ Chart 1 shows the general structures for the complexes described in the present work (**I**), and related complexes prepared by Stone (**II**), Tessier (**III**), and Osakada (**IV**). Table 4 summarizes key features observed in the spectroscopic and crystallographic data for **I–IV**.

The ^1H NMR data for **6–10** show unusually low field resonances for the terminal Si–H moiety and a high field shift for the bridging hydrides. The $^1J_{\text{SiH}}$ coupling of 48 Hz for the nonclassical interaction in **9** falls within the range of values reported for other systems containing a nonclassical type interaction.² For comparison, the bridging hydrogens in the related complex **III** ($\text{R}' = \text{Et}$) were found at $1.03\text{--}1.05$ ppm in C_6D_6 with $^1J_{\text{SiH}} = 30$ Hz.⁷ In addition, the presence of the bridging hydride was confirmed by IR spectroscopy and the $\nu(\text{Pt}\cdots\text{H}\cdots\text{Si})$ stretching values are in a close agreement with the values reported for **II**⁶ (~ 1645 cm^{-1}) and **III**⁷ (~ 1630 cm^{-1}). The fluxional behavior found in complexes **6–8** is unusual and was not observed in the related com-

(29) Green, M.; Howard, J. A. K.; Proud, J.; Spencer, J. L.; Stone, F. G. A.; Tsepis, C. *J. Chem. Soc., Chem. Commun.* **1976**, 671.

(30) The mean value for terminal (1.61 Å) and bridging Pt–H (1.69 Å) distances were determined by neutron diffraction: Bau, R.; Drabnis, M. H. *Inorg. Chim. Acta* **1997**, 259, 27.

Table 4. Selected Spectroscopic and X-ray Crystallographic Data for I–IV

	I ^a	II ^{a,b}	III ^{a,c}	IV ^{a,d}
¹ H NMR ^e				
terminal Si–H	8.4–8.9			
bridging Si–H	0.4–2.4	1.89	1.03–1.05	1.07–1.77
¹ J _{SiH} (bridging)	48 (for 9)		30	77–78
¹ J _{PtH} (bridging)	650	608		
³¹ P NMR ^e				
	37.7–41.2	35.8–57.8	23.6	–34 to +15
¹ J _{PtP}	4250–4389	3971–4237	2465	
² J _{PtP}	216–305	231–319	1346	
²⁹ Si NMR ^e				
¹ J _{PtSi}	125–175		194	
			707	
IR ^f				
terminal Si–H	2102–2158			
bridging Si–H	1618–1686	1625–1655	1630	
X-ray ^g				
Pt–Si	2.29–2.43	2.32–2.42	2.34–2.44	2.33–2.39 (Pd–Si)
Pt–Pt	2.70–2.71	2.70	2.68	2.69–2.70 (Pd–Pd)
Pt···H	1.74–1.80	1.78		1.85–2.04 (Pd···H)
Si···H	1.65–1.67	1.72		1.60–1.75
Pt–Si–Pt	69–70	69	68	69–70
Si–Pt–Si	109–110	110	111–112	110

^a See Chart 1 for structure. ^b X-ray data for R' = Cy, R = Me.^c Data are listed for R' = Et. ^d Data are listed for R' = Ph, R' = Me, Et; SiR₂ = SiMePh, R' = Me; spectra obtained in CD₂Cl₂.^e Chemical shifts are given in ppm, and coupling constants are given in Hz. Spectra were obtained in C₆D₆ unless otherwise noted.^f Si–H stretching frequency reported in cm^{–1}. ^g Distances are in angstroms; angles are in degrees.

plexes **II** and **III**. However, the unsymmetrical Pd complex [(L)Pd($\mu\text{-}\eta^2\text{-H-SiR}_2$)Pd(L)]_n (L = PMe₃; R₂Si = Ph₂Si; n = 2) was fluxional by ³¹P NMR spectroscopy (involving the dissociation of one PMe₃ ligand).⁸

The ³¹P NMR data for **6–10** exhibit a typical pattern for a diplatinum system containing one phosphorus atom at each metal center. Similar data were observed by Stone et al. for the related derivatives **II**, where the chemical shifts ranged from ~36 to 58 ppm and the measured coupling constants were ¹J_{PtP} ≈ 4100 Hz and ²J_{PtP} ≈ 270 Hz.⁶ In contrast, remarkably different couplings were seen for **III** (23.6 ppm for P bound to the ring Pt; ¹J_{PtP} = 2465 Hz; ²J_{PtP} was not resolved).⁷

The ²⁹Si NMR spectra for **6–10** show resonances that are consistent with data for complexes containing bridging silylene moieties (including those with M···H···Si interactions) which exhibit resonances in the range of 60–290 ppm.^{5a,31} The nonclassical complex **III** exhibited a ²⁹Si resonance at much lower field than complexes **6–8** and **10** with a resonance at 195 ppm.⁷

Several diagnostic features are seen in the solid-state structures of **6**, **9**, and **10**. All three of these complexes show a pattern of two alternating Si–Pt distances. This trend was also observed in the molecular structure of **II** (R' = Cy; R = Me), which exhibited similar Pt–Si bond distances (2.324(2) and 2.420(2) Å).⁶ Four different ring Pt–Si distances were observed in **III** (R' = Et) with alternating shorter and longer distances in the range of 2.347(3)–2.441(4) Å.⁷ In addition, the related Pd analogues **IV** exhibited alternating Si–Pd bond lengths in the range of 2.318(2)–2.411(2) Å.⁸ Elongated M···H

and Si···H distances are expected in complexes containing a nonclassical M···H···Si interaction, and indeed this was found in complexes **6** and **9**. These distances are in close agreement with the structure reported by Stone et al. for **II** (R' = Cy; R = Me) (Pt···H = 1.78 Å and Si···H = 1.72 Å).⁶ The palladium analogues **IV** also revealed elongated Pd···H and Si···H bond lengths.⁸

Other prominent features found in the structures of **6**, **9**, and **10** are the angles associated with the ring Pt and Si atoms. Acute Pt–Si–Pt and obtuse Si–Pt–Si angles were found in all three of these structures. These angles are in agreement with those observed by Tessier and co-workers for **III** (R' = Et), which displayed Si–Pt–Si angles of 113–114° and Pt–Si–Pt angles of 66–67°.⁷ Stone et al. found Si–Pt–Si values of 110.4(3)° and Pt–Si–Pt angles of 69.5(3)° for **II** (R' = Cy; R = Me).⁶ The related Pd analogues **IV** displayed Si–Pt–Si angles of ~110° and Pd–Si–Pd values of ~69°.⁸

Mechanistic Studies. The arylsilanes **1–3** reacted instantaneously with (Ph₃P)₂Pt($\eta^2\text{-C}_2\text{H}_4$) to afford {(Ph₃P)Pt[$\mu\text{-}\eta^2\text{-H-SiH(Ar)}$]}₂ (**6–8**). No intermediates were observed, even when an attempt was made to monitor the reaction at low temperature by NMR spectroscopy. Presumably, the first step involves the oxidative addition of the silane to the Pt center to give a complex of the type (Ph₃P)₂Pt(H)(SiH₂Ar). A subsequent reaction then occurs to give the observed products **6–8**. Tetrakis(triphenylphosphine)platinum was introduced as an alternative Pt(0) precursor to (Ph₃P)₂Pt($\eta^2\text{-C}_2\text{H}_4$), with the expectation that the reaction with the silane would proceed at a slower rate, allowing the possibility of monitoring the stages of reaction by NMR spectroscopy. However, when silane **1** was treated with Pt(PPh₃)₄ at room temperature and the reaction was monitored by ³¹P NMR spectroscopy, only peaks due to free Ph₃P and product **6** (observed as a broad hump centered around 38 ppm) were detected.¹⁰

In contrast, arylsilanes **4** and **5** exhibited slower reactivity with (Ph₃P)₂Pt($\eta^2\text{-C}_2\text{H}_4$) at room temperature, initially resulting in the formation of **11** and **12**, respectively. Complex **12** was found to be stable in the solid state but decomposes in benzene and toluene solutions over time (to unidentified products). Significantly slower decomposition of **12** occurs in the reaction mixture, whereas the decomposition process is fairly rapid for a solution of the pure complex.^{24d} The reaction mixture of **12** was monitored by ¹H and ³¹P NMR over several weeks, and after several days dissociation of a phosphine ligand trans to silicon was observed. The ³¹P NMR spectrum of an aged solution of the reaction mixture containing **12** exhibited broadened peaks due to the trans phosphine, whereas the resonance due to the cis phosphine did not change its appearance relative to the freshly prepared solution. A ³¹P–³¹P EXSY experiment indicated that the free phosphine exchanged with both platinum-bound phosphines. Eventually, the peaks for the trans phosphine disappeared; however, no new Pt–Si-containing products were observed. Similarly, proton NMR spectra of aged solutions of **12** revealed much broader aromatic resonances for the trans phosphine and the fine structure in the hydride resonance was no longer observed. It should be noted that while the hydride resonance became very broad, the Si–H resonance was completely unaffected. Thus,

(31) (a) Lickiss, P. D. *Chem. Soc. Rev.* **1992**, 21, 271. (b) Zybail, C. *Top. Curr. Chem.* **1991**, 160, 1.

it appears that the reason for the greater stability of **12** in the reaction mixture in comparison to pure **12** is the presence of excess silane, which presumably slows down the decomposition process.^{32,33} Additionally, no signs of decomposition were observed when complex **12** was heated to 100 °C in toluene-*d*₈ for several days in the reaction mixture, in contrast to rapid decomposition of pure **12** at room temperature.

The slow formation of complex **10** is most likely attributed to the extraordinary stability of the initial product, *cis*-(Ph₃P)₂Pt(H)[SiH₂(R_F)] (**12**), in contrast to *cis*-(Ph₃P)₂Pt(H)(SiH₂Ar) (Ar = IMP, TMP, Mes), which were not observed even at low temperatures. Even though slightly aged solutions of **12** (ca. 12 h) exhibited small resonances attributed to free Ph₃P and **10** (by ³¹P-{¹H} NMR), the conversion of **12** to **10** by NMR to any significant extent was not observed. The results described above suggest that phosphine loss from a species analogous to **11** and **12** may be the initial step in the mechanism of formation of the dinuclear complexes **6–10**. The precise mechanism of formation of **6–10** is unknown at the present time.

Summary

The formation of complexes of the type {(Ph₃P)Pt[μ-η²-H-SiH(Ar)]₂} (**6–10**) was observed only in those cases where the aryl group contains ortho substituents (Ar = IMP, TMP, Mes, PPP, R_F). A different structural motif is observed when the ortho substituents are removed (Ar = *p*-Tol), resulting in the formation of a bis(silyl)platinum complex (**13**). On the other hand, removal of the para substituents (i.e., IMP vs Mes) did not seem to influence the reactivity of the silane precursor or the nature of the product formed. These initial results found with the R_F ligand system at silicon suggest that the electronic character of the groups on the silane (and possibly Pt) have a significant impact on the formation of the dinuclear complexes **6–10**. The current study has shown that altering the substituents at the silane results in the formation of Pt–Si complexes of differing structural types. Recent work has also shown that alteration of the phosphine substituents at the Pt center influences the outcome of the reaction of bulky monoarylsilanes with platinum phosphine precursors.^{5b} Further studies are needed to resolve the mode of formation of complexes **6–10** (such as steric and/or electronic effects at silicon and platinum).

Experimental Section

General Materials and Procedures. All reactions and manipulations were performed in dry glassware under an argon atmosphere in an inert-atmosphere drybox or on a double-manifold Schlenk line. All solvents were distilled under an atmosphere of N₂ and dried before use: pentanes, hexanes, and C₆H₆ (CaH₂); Et₂O and DME (sodium/benzophenone ketyl); THF (CaH₂, then sodium/benzophenone ketyl). Solvents were degassed by freeze–pump–thaw degassing (liquid N₂) before being brought into the drybox. Toluene-*d*₈, CD₂Cl₂, and C₆D₆ were dried over activated alumina and Linde molecular sieves

(4 Å) before use. Pt(PPh₃)₄ (Strem Chemical) and (Ph₃P)₂Pt-(η²-C₂H₄) (Aldrich Chemical Co.) were used as received. {(Ph₃P)Pt[μ-η²-H-SiH(IMP)]₂} (**6**) was previously prepared by reaction of IMPSiH₃ (**1**) with (Ph₃P)₂Pt(η²-C₂H₄).¹⁰ (*p*-Tol)SiH₃ was prepared by reduction of commercially available (*p*-Tol)-SiCl₃ (Aldrich Chemical Co.) with LiAlH₄ in Et₂O at 0 °C.³⁴ The syntheses of the hydrosilanes TMPSiH₃,¹¹ MesSiH₃,¹² PPPSiH₃,¹³ and R_FSiH₃¹⁴ were reported elsewhere.

All NMR data were recorded on either a Bruker ARX-500 MHz spectrometer or Varian Unity Plus 300 MHz WB spectrometer at ambient temperature (unless noted otherwise). Chemical shifts (δ) are reported in ppm and coupling constants (*J*) in hertz. Because of the low solubility of **6–10**, fairly long NMR acquisition times were required which prevented determination of all coupling constants. The solution ²⁹Si spectra were acquired using the DEPT pulse sequence³⁵ or a 2D ¹H–²⁹Si HMQC³⁶ experiment. Infrared spectra were recorded on a Perkin-Elmer 1600 series FT-IR spectrometer. High-resolution mass spectra were measured at the Washington University Resource for Biomedical and Bioorganic Mass Spectrometry, and parent ion or highest mass peaks are reported. Elemental analyses were obtained from Atlantic Microlab, Inc., Norcross, GA. X-ray crystal structure determinations were performed on a Bruker SMART diffractometer equipped with a CCD area detector at 233 K.

Variable-Temperature NMR Spectroscopy of 6. A sample of **6** (4 mg, 3.2 × 10⁻⁶ mol) was dissolved in 1 mL of toluene-*d*₈ and analyzed by ¹H NMR from room temperature (25 °C) to 75 °C in 10 °C increments and from 66 to 75 °C in 1 °C increments to determine the coalescence temperature for the terminal Si–H resonances of **6a** and **6b** (8–9 ppm). The coalescence temperature (*T*_c) was found to be 69 °C.

Preparation of {(Ph₃P)Pt[μ-η²-H-SiH(TMP)]₂} (7**).** A solution of (TMP)SiH₃ (**2**; 30 mg, 0.15 mmol) was added to a 7 mL vial containing (Ph₃P)₂Pt(η²-C₂H₄) (98 mg, 0.13 mmol) in 1 mL of C₆H₆. Vigorous evolution of gas was observed, and the color of the reaction mixture turned from yellow to amber. After 1 h precipitation of a microcrystalline white solid (**7**) was observed. After 24 h the solid was filtered, washed with Et₂O (6 × 0.5 mL), and then dried in vacuo to give {(Ph₃P)Pt[μ-η²-H-SiH(TMP)]₂} (**7**; 68 mg, 79% yield) as a mixture of *trans* (**7a**) and *cis* (**7b**) isomers (ratio 3:2 by NMR). ¹H NMR (C₆D₆, 300 MHz) for **7a**: δ 2.44 (bd, 2H, ²*J*_{PtH} = 118 Hz, ¹*J*_{PtH} not resolved, Pt···H···Si), 3.03 (s, 12H, *o*-ArOCH₃), 3.40 (s, 6H, *p*-ArOCH₃),³⁷ 5.94 (s, 4H, Ar *H*), 6.95 [m, 18H, P(*m*-C₆H₅)₃ and P(*p*-C₆H₅)₃], 7.79 [m, 12H, P(*o*-C₆H₅)₃], 8.95 (s, 2H, ²*J*_{PtH} = 159 Hz, ²*J*_{PtH} = 74 Hz, SiH). ²⁹Si{¹H} NMR (C₆D₆, ¹H–²⁹Si HMQC, 500 MHz): δ 125. IR (KBr, cm⁻¹): ν 2102.0 (Si–H), ~1634 (Pt–H, partially overlaps with C=C stretching). Anal. Calcd for C₅₄H₅₆O₆ P₂Pt₂Si₂: C, 49.54; H, 4.31. Found: C, 49.12; H, 4.34. ¹H NMR (C₆D₆, ppm, 300 MHz) for **7b**: δ 2.38 (bd, 2H, Pt···H···Si, coupling constants not resolved), 3.00 (s, 12H, *o*-ArOCH₃), 3.40 (s, 6H, *p*-ArOCH₃), 5.88 (s, 4H, Ar *H*), 6.95 [m, 18H, P(*m*-C₆H₅)₃ and P(*p*-C₆H₅)₃], 7.79 [m, 12H, P(*o*-C₆H₅)₃], 8.65 (s, 2H, SiH), ²*J*_{PtH} = 160 Hz, ²*J*_{PtH} = 79 Hz). ²⁹Si{¹H} NMR (C₆D₆, ¹H–²⁹Si HMQC, 500 MHz): δ 126. IR (KBr, cm⁻¹): ν 2102.0 (Si–H), ~1634 (Pt–H, partially overlaps with C=C stretching).

Variable-Temperature NMR Spectroscopy of 7. A sample of **7** (4 mg, 3.1 × 10⁻⁶ mol) was dissolved in 1 mL of toluene-*d*₈ and analyzed by VT-NMR. The sample was analyzed by ¹H NMR from room temperature (25 °C) to 75 °C in 10 °C increments and from 68 to 70 °C in 1 °C increments to determine the coalescence temperature for the terminal Si–H

(32) Several reports show examples of transition-metal–silyl species that are stable only in the presence of excess silane. See, for example, ref 24d.

(33) An ¹H–¹H EXSY experiment revealed that **12** undergoes exchange when excess R_FSiH₃ is present.

(34) Banovets, J. P.; Suzuki, H.; Waymouth, R. M. *Organometallics* **1993**, *12*, 4700.

(35) Blinka, T. A.; Helmer, B. J. *Adv. Organomet. Chem.* **1984**, *23*, 193.

(36) Bax, A.; Subramanian, S. *J. Magn. Reson.* **1986**, *67*, 565.

(37) Overlaps with the *cis* isomer **7b**.

resonances of **7a** and **7b** (8–9 ppm). The coalescence temperature (T_c) was found to be 70 °C (343 K).

Preparation of $\{(\text{Ph}_3\text{P})\text{Pt}[\mu\text{-}\eta^2\text{-H-SiH(Mes)}]\}_2$ (8**).** In a 7 mL vial containing MesSiH₃ (**3**; 24 mg, 0.16 mmol) were added (Ph₃P)₂Pt(η^2 -C₂H₄) (98 mg, 0.13 mmol) and 3 mL of C₆H₆. Vigorous gas evolution was observed, and the solution turned bright yellow. After approximately 24 h a small amount of off-white solid, $\{(\text{Ph}_3\text{P})\text{Pt}[\mu\text{-}\eta^2\text{-H-SiH(Mes)}]\}_2$ (**8**), had formed, which was washed with Et₂O (2 × 1 mL) and dried in vacuo. Additional solid was obtained from the mother liquor and washed with Et₂O and dried. Total yield of **8**: 56 mg, 71% as a mixture of trans (**8a**) and cis (**8b**) isomers (ratio 3:2 by NMR). ¹H NMR (C₆D₆, 300 MHz) for **8a**: δ 2.14 (s, 6H, *p*-ArCH₃), 2.27 (bd, 2H, ¹*J*_{PH} = 650 Hz, ²*J*_{PH} = 5 Hz, ²*J*_{PH} not resolved, Pt···H···Si), 2.38 (s, 12H, *o*-ArCH₃), 6.61 (s, 4H, Ar *H*), 6.89 [m, 18H, P(*m*-C₆H₅)₃ and P(*p*-C₆H₅)₃], 7.61 [m, 12H, P(*o*-C₆H₅)₃], 8.95 (s, 2H, ²*J*_{PH} = 136 Hz, ²*J*_{PH} = 75 Hz, SiH). ²⁹Si{¹H} NMR (C₆D₆, ¹H-²⁹Si HMQC, 500 MHz): δ 131. IR (KBr, cm⁻¹): ν 2122.3 (Si-H), 1618.0 (Pt-H). Anal. Calcd for C₅₄H₅₆P₂Ti₂Si₂: C, 53.46; H, 4.65. Found: C, 52.99; H, 4.69. ¹H NMR (C₆D₆, ppm, 300 MHz) for **8b**: δ 2.17 (s, 6H, *p*-ArCH₃), 2.34 (s, 12H, *o*-ArCH₃), 6.68 (s, 4H, Ar *H*), 6.89 [m, 18H, P(*m*-C₆H₅)₃ and P(*p*-C₆H₅)₃], 7.61 [m, 12H, P(*o*-C₆H₅)₃], 8.52 (s, 2H, ²*J*_{PH} = 135 Hz, ²*J*_{PH} = 73 Hz, SiH). ³¹P{¹H} NMR (C₆D₆, 121 MHz): δ 38.2 (¹*J*_{PP} = 4264 Hz, ²*J*_{PP} = 252 Hz, ³*J*_{PP} = 60 Hz). ²⁹Si{¹H} NMR (C₆D₆, ¹H-²⁹Si HMQC, 500 MHz): δ 129. IR (KBr, cm⁻¹): ν 2116.1 (Si-H), 1618.0 (Pt-H).

Variable-Temperature NMR Spectroscopy of **8.** A sample of **8** (4 mg, 5.8 × 10⁻⁶ mol) was dissolved in 1 mL of toluene-*d*₈ and analyzed by ¹H NMR spectroscopy from room temperature (25 °C) to 95 °C in 10 °C increments and from 77 to 83 °C in 2 °C increments to determine the coalescence temperature for the terminal Si-H resonances of **8a** and **8b** (8–9 ppm). The coalescence temperature (T_c) was found to be 83 °C (356 K).

Preparation of $\{(\text{Ph}_3\text{P})\text{Pt}[\mu\text{-}\eta^2\text{-D-SiD(Mes)}]\}_2$ (8-d**).** In a 7 mL vial containing 52 mg (0.07 mmol) of (Ph₃P)₂Pt(η^2 -C₂H₄) was placed a solution of MesSiD₃ (**3-d**; 13 mg, 0.08 mmol) in C₆H₆ (1 mL). Rapid gas evolution was observed, the solution turned pale yellow, and a solid precipitate formed after 3 h. After 24 h the solid was filtered, washed with Et₂O (8 × 1 mL), and then dried in vacuo to give 28 mg of $\{(\text{Ph}_3\text{P})\text{Pt}[\mu\text{-}\eta^2\text{-D-SiD(Mes)}]\}_2$ (**8-d**), (67% yield) as a mixture of trans (**8a-d**) and cis (**8b-d**) isomers (ratio 3:2 by NMR). ¹H NMR (C₆D₆, 300 MHz) for **8a-d**: δ 2.14 (s, 6H, *p*-ArCH₃), 2.38 (s, 12H, *o*-ArCH₃), 6.62 (s, 4H, Ar *H*), 6.89 [m, 18H, P(*m*-C₆H₅)₃ and P(*p*-C₆H₅)₃], 7.60 [m, 12H, P(*o*-C₆H₅)₃], ²H NMR (C₆H₆/C₆D₆, 77 MHz): δ 2.28 (b, 2D, ¹*J*_{PD} = 102 Hz, ²*J*_{PD} not resolved, Pt···D···Si), 8.93 (s, 2D, ¹*J*_{PD} not resolved, SiD). ³¹P{¹H} NMR (C₆D₆, ppm, 121 MHz): 39.0 (¹*J*_{PP} = 4251 Hz, ²*J*_{PP} = 263 Hz, ³*J*_{PP} = 56 Hz). IR (KBr, cm⁻¹): ν 1541.5 (Si-D), 1157.4 (Pt-D). Anal. Calcd for C₅₄H₅₂D₄P₂Ti₂Si₂: C, 53.29; H, 4.28. Found: C, 52.91; H, 4.67. ¹H NMR (C₆D₆, 300 MHz) for **8b-d**: δ 2.17 (s, 6H, *p*-ArCH₃), 2.33 (s, 12H, *o*-ArOCH₃), 6.68 (s, 4H, Ar *H*), 6.89 [m, 18H, P(*m*-C₆H₅)₃ and P(*p*-C₆H₅)₃], 7.60 [m, 12H, P(*o*-C₆H₅)₃], ²H NMR (C₆H₆/C₆D₆, 77 MHz): δ 1.49 (b, 2D, ¹*J*_{PD} and ²*J*_{PD} not resolved, Pt···D···Si), 8.51 (s, 2D, ²*J*_{PD} not resolved, SiD). ³¹P{¹H} NMR (C₆D₆, 121 MHz): 38.6 (¹*J*_{PP} = 4249 Hz, ²*J*_{PP} = 251 Hz, ³*J*_{PP} = 56 Hz). IR (KBr, cm⁻¹): ν 1541.5 (Si-D), 1157.4 (Pt-D).

Preparation of trans- $\{(\text{Ph}_3\text{P})\text{Pt}[\mu\text{-}\eta^2\text{-H-SiH(PPP)}]\}_2$ (9**).** A sample of (Ph₃P)₂Pt(η^2 -C₂H₄) (61 mg, 0.08 mmol) was dissolved in C₆H₆ (1.5 mL), and a solution of PPPSiH₃ (**4**; 41 mg, 0.08 mmol, 1.5 mL C₆H₆) was added. The reaction mixture turned yellow, and slow evolution of gas was observed. The solution was heated to 78 °C, and vigorous bubbling was observed immediately, followed by precipitation of trans- $\{(\text{Ph}_3\text{P})\text{Pt}[\mu\text{-}\eta^2\text{-H-SiH(PPP)}]\}_2$ (**9**) within minutes. The solid

was washed with 5 mL of C₆H₆ and 10 mL of hexanes and then dried in vacuo to afford **9** as a cream-colored solid (75 mg, 97%). ¹H NMR (CD₂Cl₂, 500 MHz): δ 0.35 (d, 2H, ¹*J*_{SiH} = 48 Hz, ²*J*_{SiH} = 25 Hz, ¹*J*_{PH} = 650 Hz, ²*J*_{PH} = 112 Hz, ²*J*_{PH} = 7 Hz, Pt-H-Si), 5.89–7.83 [m, 80H, P(C₆H₅)₃ and Si[C₆(C₆H₅)₅], 7.48 (s, 2H, Si-H). ²⁹Si{¹H} NMR (CD₂Cl₂, ¹H-²⁹Si HMQC, 500 MHz): δ 174.5. IR (KBr, cm⁻¹): ν 2118.1 (Si-H), 1654.0 (Pt-H-Si). Anal. Calcd for C₁₀₈H₈₄P₂Pt₂Si₂: C, 68.63; H, 4.48. Found: C, 68.05; H, 4.52.

Preparation of trans- $\{(\text{Ph}_3\text{P})\text{Pt}[\mu\text{-}\eta^2\text{-H-SiH(R}_F\text{)}]\}_2$ (10**).** A solution of (R_F)SiH₃ (**5**; 22 mg, 0.07 mmol) in 1 mL C₆H₆ was added to (Ph₃P)₂Pt(η^2 -C₂H₄) (52 mg, 0.07 mmol) to give a clear amber solution. Vigorous bubbling was observed initially for approximately 5 min. The reaction mixture was set aside in the drybox for 2 months, after which evaporation of the solvent had occurred to give a dark amber oily residue. The residue was extracted with Et₂O (2 mL), and the washings were stored at -35 °C for several days, after which pale yellow microcrystals of trans- $\{(\text{Ph}_3\text{P})\text{Pt}[\mu\text{-}\eta^2\text{-H-SiH(R}_F\text{)}]\}_2$ (**10**) suitable for X-ray analysis had formed. The solid was washed with cold hexanes (3 × 1 mL) and dried in vacuo to give 10 mg (19% yield) of **10**. ¹H NMR (C₆D₆, 300 MHz) for **10**: δ 2.10 (b, 2H, coupling constants not resolved, Pt···H···Si), 6.81 [m, 18H, P(*m*-C₆H₅)₃ and P(*p*-C₆H₅)₃], 7.57 [m, 12H, P(*o*-C₆H₅)₃], 7.68 (bs, 4H, Ar *H*), 8.41 (m, 2H, coupling constants not resolved, SiH). ²⁹Si{¹H} NMR (C₆D₆, ¹H-²⁹Si HMQC, 500 MHz): δ 135. IR (KBr, cm⁻¹): ν 2158.4 (Si-H), 1686.0 (Pt-H). Anal. Calcd for C₅₄H₃₈F₁₈P₂Pt₂Si₂: C, 42.19; H, 2.49. Found: C, 39.65; H, 2.38.

Preparation of cis- $\{(\text{Ph}_3\text{P})_2\text{Pt(H)[SiH}_2\text{(PPP)]}\}$ (11**).** A solution of PPPSiH₃ (**4**; 84 mg, 0.17 mmol) in 1.0 mL of C₆D₆ was added to (Ph₃P)₂Pt(η^2 -C₂H₄) (131 mg, 0.17 mmol) to give a clear amber solution with vigorous bubbling for approximately 5 min. Analysis of the reaction mixture by ¹H and ³¹P{¹H} NMR indicated quantitative formation of cis- $\{(\text{Ph}_3\text{P})_2\text{Pt(H)[SiH}_2\text{(PPP)]}\}$ (**11**). After 1 h an off-white solid began to precipitate. The solution was filtered, and the solid was washed with 4 mL of C₆H₆ and dried in vacuo to give 157 mg (76%) of **11**. ¹H NMR (C₆D₆, 300 MHz): δ -1.81 [dd, 1H, ²*J*_{PH} = 21 Hz (cis), ²*J*_{PH} = 156 Hz (trans), ¹*J*_{PH} = 984 Hz, Pt-H], 4.26 (pt, 2H, ¹*J*_{SiH} = 182 Hz, ³*J*_{PH} = 7 Hz, Si-H), 6.65–7.60 [m, 55H, P(C₆H₅)₃ and Si[C₆(C₆H₅)₅]. ³¹P{¹H} NMR (C₆D₆, 121 MHz): 31.7 (d, ¹*J*_{PP} = 1713 Hz, ²*J*_{PP} = 14 Hz, PtP *trans* to Si), 32.9 (d, ¹*J*_{PP} = 2422 Hz, ²*J*_{PP} = 14 Hz, PtP *cis* to Si). ²⁹Si{¹H} NMR (C₆D₆, DEPT, 99 MHz): δ -45.7 [dd, ¹*J*_{PSi} = 1155 Hz, ²*J*_{PSi} = 155 Hz (trans), ²*J*_{PSi} = 12 Hz (cis)]. IR (KBr, cm⁻¹): ν 2088.8 (Si-H), 2067.6 (Pt-H). Anal. Calcd for C₇₂H₅₈P₂PtSi: C, 71.57; H, 4.84. Found: C, 69.77; H, 4.72.

Preparation of cis- $\{(\text{Ph}_3\text{P})_2\text{Pt(H)[SiH}_2\text{(R}_F\text{)}]\}$ (12**).** A solution of (R_F)SiH₃ (**5**; 22 mg, 0.07 mmol) in 1 mL of C₆H₆ was added to (Ph₃P)₂Pt(η^2 -C₂H₄) (48 mg, 0.06 mmol) to give a clear yellow solution. Vigorous bubbling was observed initially for approximately 5 min, and then hexanes (ca. 5 mL) were added to the reaction mixture. The solution was stored at -35 °C for several days, after which pale yellow microcrystals of cis- $\{(\text{Ph}_3\text{P})_2\text{Pt(H)[SiH}_2\text{(R}_F\text{)}]\}$ (**12**) had formed. The solid was washed with hexanes (3 × 3 mL) and dried in vacuo to give 36 mg (54% yield)³⁹ of **12**. ¹H NMR (C₆D₆, 500 MHz): δ -2.39 [dd, 1H, ²*J*_{PH} = 20 Hz (cis), ²*J*_{PH} = 156 Hz (trans), ¹*J*_{PH} = 930 Hz, Pt-H], 5.03 (m, 2H, ¹*J*_{SiH} = 187 Hz, ²*J*_{PH} = 20 Hz, ⁵*J*_{PH} = 8 Hz, Si-H), 6.86 [m, 9H, P(*m*-C₆H₅)₃ and P(*p*-C₆H₅)₃ *trans* to Si], 6.89 [m, 9H, P(*m*-C₆H₅)₃ and P(*p*-C₆H₅)₃ *cis* to Si], 7.44 [m, 6H, P(*o*-C₆H₅)₃ *trans* to Si], 7.52 [m, 6H, P(*o*-C₆H₅)₃ *cis* to Si], 7.86 (s, 2H, Ar *H*). ¹⁹F NMR (C₆D₆, 471 MHz): δ -63.3 (s, 3F, ⁷*J*_{PF} = 11 Hz, *p*-CF₃), -57.2 (dt, 6F, ⁵*J*_{SiHF} = 8 Hz, ⁵*J*_{PF} = 64 Hz, ⁶*J*_{PHF} = 2 Hz, *o*-CF₃). ²⁹Si{¹H} NMR (C₆D₆, DEPT, 99 MHz): δ -45.1 [dm, ¹*J*_{PSi} = 1326 Hz, ²*J*_{PSi} = 175 Hz (trans),

(38) Only terminal Si-H could be observed for **8b**. The bridging Si-H resonance was obscured by the ArMe group.

(39) The reaction was quantitative by ¹H and ³¹P NMR spectroscopy. A low isolated yield of **12** is probably due to loss of product during workup.

$^2J_{\text{PSi}}$ (cis), J_{SiF} are not resolved]. $^{31}\text{P}\{^1\text{H}\}$ NMR (C_6D_6 , 121 MHz): 30.3 (d, $^1J_{\text{PtP}} = 1896$ Hz, $^2J_{\text{PP}} = 16$ Hz, PtP *trans* to Si), 30.6 (d, $^1J_{\text{PtP}} = 2282$ Hz, $^2J_{\text{PP}} = 16$ Hz, PtP *cis* to Si). IR (KBr, cm^{-1}): ν 2125.5 (Si–H), 2071.6 (Pt–H). Anal. Calcd for $\text{C}_{45}\text{H}_{35}\text{F}_9\text{P}_2\text{PtSi}$: C, 52.38; H, 3.39. Found: C, 51.82; H, 3.41.

Preparation of *cis*-(Ph_3P) $_2\text{Pt}[\text{SiH}_2(p\text{-Tol})]_2$ (13**).** A sample of $(\text{Ph}_3\text{P})_2\text{Pt}(\eta^2\text{-C}_2\text{H}_4)$ (53 mg, 0.07 mmol) was treated with a solution of $(p\text{-Tol})\text{SiH}_3$ (22 mg, 0.18 mmol) in toluene- d_8 (1 mL) to give a yellow solution. Bubbling was observed for about 5 min, and analysis of the sample by ^1H and $^{31}\text{P}\{^1\text{H}\}$ NMR indicated quantitative formation of *cis*-(Ph_3P) $_2\text{Pt}[\text{SiH}_2(p\text{-Tol})]_2$ (**13**). Precipitation of **13** was achieved by addition of hexanes (2.5 mL), followed by storage at -35°C (2.5 h in the dark). The solution was filtered, and the yellow solid was dried in vacuo to give 58 mg (88%) of **13**. The clear yellow decantate was found to be light sensitive. Upon exposure to light for 10 min, the color of the decantate changed to a dark amber. In addition, the yellow solid was sensitive to light and changed from yellow to orange upon exposure for 5 min. ^1H NMR (C_6D_6 , 300 MHz): δ 2.20 (s, 6H, ArCH_3), 5.08 (m, 4H, $^1J_{\text{SiH}} = 177$ Hz, $^2J_{\text{PSiH}} = 53$ Hz, $^3J_{\text{PSiH}} = 14$ Hz, SiH), 6.87 [m, 18H, $\text{P}(m\text{-C}_6\text{H}_5)_3$ and $\text{P}(p\text{-C}_6\text{H}_5)_3$], 7.07 (d, 4H, $^3J_{\text{HH}} = 7$ Hz, Ar H), 7.39 [m, 12H, $\text{P}(o\text{-C}_6\text{H}_5)_3$], 7.77 (d, 4H, $^3J_{\text{HH}} = 7$ Hz, Ar H). $^{31}\text{P}\{^1\text{H}\}$ NMR (C_6D_6 , 121 MHz): δ 35.5 [$^1J_{\text{PtP}} = 1887$ Hz, $^2J_{\text{PSi}} = 21$ Hz (cis), $^2J_{\text{PSi}} = 62$ Hz (trans)].

X-ray Crystallography. Crystals of **9** were grown from a dilute C_6D_6 solution by slow evaporation over several days. Crystals of **10** were grown from Et_2O at -35°C over a period of several days. Preliminary examination and data collection were performed using a Bruker SMART CCD detector system. Preliminary unit cell constants were determined with a set of 45 narrow frames (0.3° in φ) scans. The data sets collected consisted of 4028 frames with a frame width of 0.3° in φ and counting time of 15 s/frame at a crystal to detector distance of 4.930 cm. The double-pass method of scanning was used to exclude any noise. SMART and SAINT software packages⁴⁰ were used for data collection and data integration. Analysis of the integrated data did not show any decay. Final cell constants were determined by a global refinement of xyz centroids. Collected data were corrected for systematic errors using SADABS⁴¹ based on the Laue symmetry using equivalent reflections.

Crystal data and intensity data collection parameters are listed in Table 1 (see also Tables S1 and S6 in the Supporting

Information). Structure solution and refinement were carried out using the SHELXTL-PLUS software package.⁴⁰ The structures were solved by direct method and refined successfully in the space group $P\bar{1}$. Full-matrix least-squares refinement was carried out by minimizing $\sum w(F_o^2 - F_c^2)^2$. The non-hydrogen atoms were refined anisotropically to convergence. The hydrogen atoms were treated using the appropriate riding model. One and a half molecules of benzene were found in the crystal lattice for compound **10**. One of the CF_3 groups is also disordered, which was resolved to be in the ratio of 75:25. In both cases the bridging H atom was located and refined successfully. Structure refinement parameters are listed in Table 2 for **10**. A projection view of the molecules with non-hydrogen atoms represented by 50% probability ellipsoids, showing the atom labeling, is presented in Figures 5 and 6.

Complete listings of the atomic coordinates for the non-hydrogen atoms and the geometrical parameters, positional and isotropic displacement coefficients for hydrogen atoms, and anisotropic displacement coefficients for the non-hydrogen atoms have been submitted as Supporting Information.

Acknowledgment. This work was supported by a University of Missouri–St. Louis Research Award. The NSF (Grant No. CHE-9318696) and the University of Missouri Research Board are gratefully acknowledged for support of the purchase of Varian Unity Plus 300 and Bruker ARX-500 NMR spectrometers. The UM–St. Louis X-ray Crystallography Facility is funded in part by a NSF Instrumentation Grant (Grant No. CHE-9309690) and a UM–St. Louis Research Award. J.B.–W. is also grateful to Professors Claire Tessier, Joyce Y. Corey, and Peter P. Gaspar for stimulating discussions.

Supporting Information Available: Tables giving additional crystallographic data for **9** and **10** and figures giving 2D NMR data for **7**, IR spectra for **8** and **8-d**, 1D and 2D NMR data for **12**, and the molecular structure of **9** showing full atom labeling. This material is available free of charge via the Internet at <http://pubs.acs.org>.

OM000602R

(40) Sheldrick, G. M. Bruker Analytical X-ray Division, Madison, WI, 1999.

(41) Blessing, R. H. *Acta Crystallogr.* **1995**, *A51*, 33.